ELSEVIER

1 September 1995

Chemical Physics Letters 242 (1995) 617–622

CHEMICAL PHYSICS LETTERS

Surface femtochemistry of O_2 and CO on Pt(111)

S. Deliwala, R.J. Finlay, J.R. Goldman, T.H. Her, W.D. Mieher, E. Mazur

Department of Physics and Division of Applied Sciences, Harvard University, Cambridge, MA 02138, USA

Received 25 May 1995

Abstract

Desorption of O_2 and formation of CO_2 were induced with subpicosecond laser pulses on a Pt(111) surface dosed with coadsorbed O_2 and CO. We report the fluence dependent yields obtained over a range of laser wavelengths from 267 to 800 nm, and pulse durations from 80 fs to 3.6 ps. The nonlinear dependence of the yield on fluence is different at different wavelengths. Two-pulse correlation measurements show two different time-scales relevant to the desorption. The results show that nonthermalized electrons play a role in the surface chemistry, and that an equilibrated pre-heating of the surface modes leads to enhanced desorption.

Recent experiments examining the desorption of adsorbed molecules from metal surfaces using subpicosecond laser pulses have shown a highly nonlinear dependence of the desorption yield on the laser fluence (energy per unit area) [1–5]. These results are in sharp contrast to those found with nanosecond or continuous irradiation where the desorption yield is linear in the fluence [6–8]. Using surface second-harmonic generation as a probe, it was shown that the ultrafast-laser-induced desorption of CO from Cu(111) takes less than 325 fs [9]. Two-pulse correlation measurements on a number of other systems show a transient excitation responsible for desorption lasting about a picosecond [2,4,5]. For comparison, the time scale for the cooling of the electrons at the surface is 1–3 ps [2,5,9,10]. Following subpicosecond laser excitation the electron temperature easily reaches several thousand kelvin because the electronic heat capacity in metals is small [11–14]. Both the nonlinear fluence dependence and the short time scale of the desorption have been attributed to hot electrons in the metal [1–5,9,10,15–17].

In this Letter, we report on the desorption of O_2 and formation of CO_2 induced with subpicosecond laser pulses on a Pt(111) surface prepared with coadsorbed CO and O_2 at 90 K. CO_2, produced on the surface in a laser-induced reaction, desorbs and is detected using a mass spectrometer. The O_2/Pt(111) and CO/O_2/Pt(111) systems have been well characterized [6,7,18–20]. The photochemistry of these systems has been studied with arc lamp irradiation [6,7], and with nanosecond [3,8] and subpicosecond [3,4] laser pulses. We report the fluence dependence of the desorption yield of O_2 and CO_2 at 267, 400, and 800 nm over a range of pulsewidths from 80 fs to 3.6 ps. The experiments presented in this Letter extend the range of excitation conditions used in previously published studies. We also present two-pulse correlation data obtained with 80 fs pulses at 800 nm using delays up to 75 ps. The results present

Elsevier Science B.V.
SSDI 0009-2614(95)00791-1

convincing evidence that nonthermalized highly excited electrons play a significant role in the desorption and surface reaction processes.

The single crystal Pt(111) surface of the 10 mm diameter sample is cleaned in an ultrahigh vacuum (UHV) chamber following published procedures [7]. The cleaned Pt surface is kept at 90 K at a base pressure of 7×10^{-11} Torr. After cleaning it is first dosed to saturation (0.44 monolayer) [21] with $^{18}O_2$ using a capillary array to minimize the O_2 background in the chamber. This dosing is followed by a 3 Langmuir background exposure (3×10^{-6} Torr s) of $^{12}C^{18}O$. Below 100 K, O_2 has been reported to chemisorb molecularly in atop and bridge sites with the O–O bond axis parallel to the surface and a bond order of about 1 [21]. The CO occupies only the atop sites in the presence of preadsorbed O_2 [7].

The laser system, consisting of a Ti:sapphire oscillator and a chirped-pulse-regenerative amplifier, produces 0.5 mJ pulses of 70 fs duration at 800 nm at a 1 kHz repetition rate. Longer pulses are obtained by adjusting the pulse compressor; this stretches the pulse in time by imposing a frequency chirp but preserves the spectral bandwidth. Frequency-doubled 400 nm pulses are produced in a 1 mm long LBO crystal yielding 0.1 mJ pulses of 0.2 ps duration. Sum-frequency mixing of the 800 and 400 nm pulses in a 0.3 mm long BBO crystal, yields 10 μJ pulses at 267 nm. Based on the group velocities of the 400 and 800 nm pulses in BBO, we estimate a pulsewidth of 0.35 ps for the 267 nm pulses.

For each data run we calibrate the fluence by measuring the energy and spatial profile of the laser pulses. The energy E is measured with a photodiode referenced to a calibrated pyroelectric detector. Typical shot-to-shot energy fluctuations are 2% at 800 nm, 5% at 400 nm, and 20% at 267 nm. We measure the profile of the 800 and 400 nm pulses with a CCD camera; no profile was measured at 267 nm. The profile is fit with an elliptical Gaussian function, and the fluence F follows from

$$E = \int\int F(\boldsymbol{r})\, \mathrm{d}\boldsymbol{r} = \int\int F \exp\left[-\left(\frac{x^2}{a^2} + \frac{y^2}{b^2}\right)\right] \mathrm{d}x\, \mathrm{d}y, \qquad (1)$$

where $F(\boldsymbol{r})$ is the fluence spatial profile with x and y the spatial coordinates in the plane of the sample; a and b are determined from a fit to the measured profile. For all wavelengths the absorbed fluence (i.e. the incident fluence times the absorption of platinum [22]) is in the range 20–160 $\mu J/mm^2$. The fluence is varied by changing the total incident energy with a half-wave plate and a polarizer.

Desorption yields at a given fluence, wavelength, and pulse width are obtained in runs of 200 laser shots on a fixed spot on the sample. Between runs the sample is translated by 0.6 mm (twice the Gaussian FWHM of the irradiated area). When the entire sample has been used, the sample is cleaned and redosed. The molecules desorbed by the laser pulse are detected with a quadrupole mass spectrometer [1]. A negatively biased grid in front of the mass spectrometer shields the sample from stray electrons from the ionizer. A mechanical shutter is used to increase the time interval between successive laser shots to 0.4 s to allow the mass spectrometer signal to return to the background. For each laser shot we record the energy of the laser and the integrated mass spectrometer signal.

Fig. 1 shows the desorption of O_2 and CO_2 at 400 and 800 nm. Each curve corresponds to a data run on a single spot. In a given run the desorption yield on subsequent laser shots decreases because the adsorbate layer is depleted. To compare runs we plot the desorption yield per unit area, $Y/\pi ab$, i.e. the yield divided by the irradiated surface area. Note that the desorption yield on the first laser shot depends nonlinearly on the fluence: as the fluence is increased from 0.05 to 0.1 mJ/mm^2, the signal obtained at 800 nm increases by considerably more than a factor of ten.

Fig. 2 shows the desorption yield per unit area on the first shot of each data run at 400 nm (0.2 ps) and 800 nm (80 fs, 0.6 ps, 3.6 ps). Fig. 3 shows the nonlinear dependence of the yield of O_2 and CO_2 on incident laser energy at 267 nm (0.35 ps). The nearly identical fluence dependence of the O_2 and CO_2 data provides strong evidence for a common excitation mechanism for desorption of O_2 and formation of

[1] UTI 100C operating in pulse counting mode.

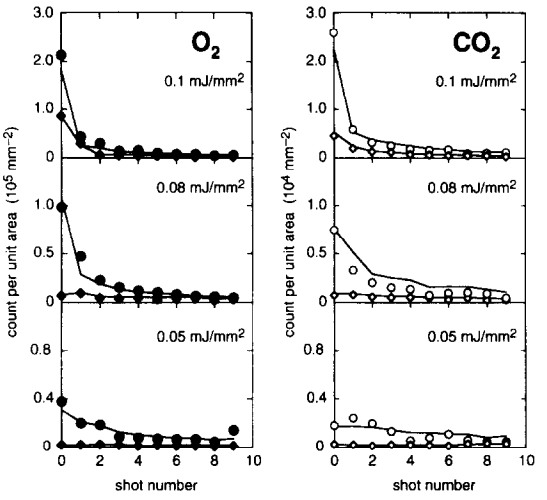

Fig. 1. Laser-induced O_2 desorption from O_2/Pt(111) (left) and CO_2 formation from CO/O_2/Pt(111) (right) for multiple laser shots on the same spot at 800 nm (◆◇) and 400 nm (●○). The curves are fits of Eq. (4) to the data. For each wavelength, one set of parameters describes the desorption yield over two decades.

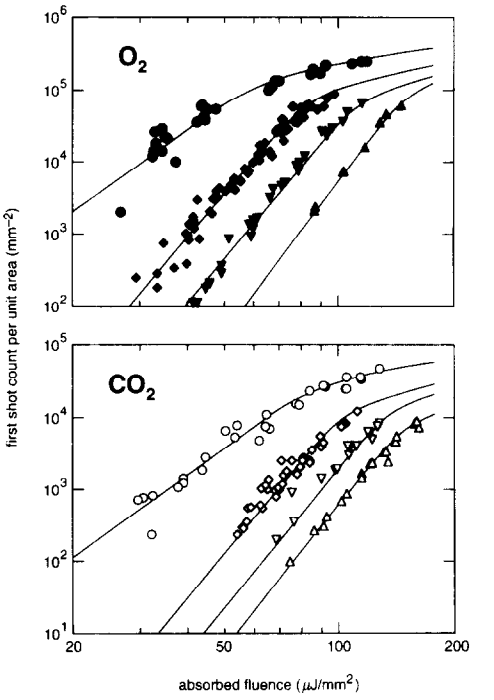

Fig. 2. First-shot O_2 desorption yield (top) and CO_2 formation yield (bottom) versus fluence for 800 nm at 80 fs (◆◇), 0.6 ps (▼▽), and 3.6 ps (▲△), and for 400 nm at 0.2 ps (●○). The curves represent Eq. (4) with the fitting parameters obtained from the depletion curves. The nonlinear desorption yield is well described by a power law dependence on the laser pulse fluence. The power law exponents are 6.5 ± 0.4 at 800 nm (for all pulse durations) and 3.8 ± 0.5 at 400 nm.

CO_2. The ratio in desorption yield of O_2 to CO_2 is about 10, in sharp contrast with the ratio of 0.5 found with nanosecond irradiation [3]. Both of these ratios are uncorrected for the relative detection efficiencies, but were obtained with the same model of mass spectrometer.

Recently published models of desorption induced by subpicosecond laser pulses assume that the excited electrons that interact with the adsorbates have a Fermi–Dirac distribution [2,4,9,16,17]. In these models, the calculated transient electron temperature depends on absorbed fluence and pulse duration but not on photon energy. However, the data in Figs. 2 and 3 show a clear dependence of desorption yield on wavelength. Consequently our data do not support the assumption that a thermalized electron distribution solely governs the desorption. This leads us to conclude that nonthermalized electrons play a role in surface reactions induced by subpicosecond laser pulses. Since electrons thermalize in less than a picosecond, a short time scale for the excitation process follows naturally. Electron equilibration times as long as a few hundred femtoseconds indeed have been observed in gold [23], but similar measurements are not available for platinum.

The data taken at 800 nm with different pulse durations show that for both O_2 and CO_2 the yield falls sharply with increasing pulse duration. To fur-

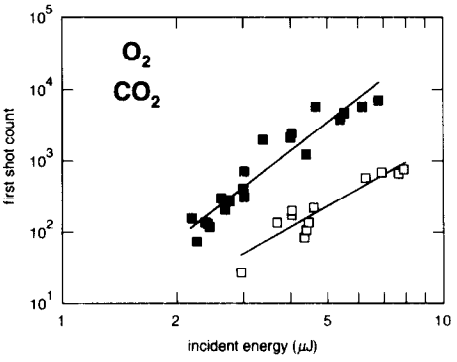

Fig. 3. First-shot O_2 desorption (■) and CO_2 reaction (□) yields induced by 267 nm (0.35 ps) pulses. The power law exponents are 4.1 and 3.0 for O_2 and CO_2, respectively.

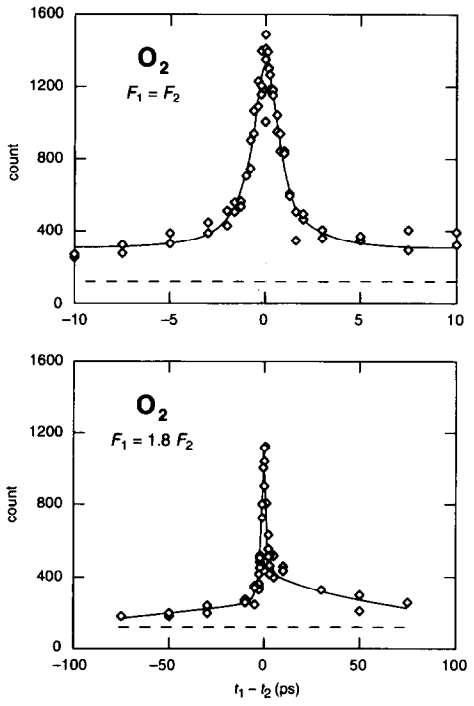

Fig. 4. Desorption yield versus time delay $t_1 - t_2$ between two 80 fs excitation pulses at 800 nm for pulses of equal (top) and unequal (bottom) absorbed fluences. The dashed lines denote $Y(t_1 - t_2 = \pm\infty)$. In both cases the width of the central peak is 1.8 ps. For unequal fluences the desorption yield is enhanced when the weaker pulse arrives first ($t_1 - t_2 > 0$). The desorption yield is still enhanced after 75 ps.

ther explore the time dependence, we measured the total desorption yield of two 80 fs laser pulses as a function of the delay $t_1 - t_2$ between them. The pulses are orthogonally polarized to avoid interference. Two examples of such traces are shown in Fig. 4, one for pulses of equal absorbed fluence, the other for pulses of unequal fluences. The dashed line shows the total yield when the two pulses act independently, i.e. when $t_1 - t_2 \rightarrow \pm\infty$. The dependence of the signal on $t_1 - t_2$ reflects the evolution of the substrate and adsorbate excitations responsible for desorption.

The data show a 1.8 ps wide peak centered at $t_1 - t_2 = 0$ on top of broad wings that are asymmetric in amplitude when the two pulses are of unequal fluence. Both the central peak and the asymmetry in the wings are in agreement with previous observations [2,4,5]. The central peak was attributed to the cooling of the hot substrate electrons which are strongly coupled to the vibrations of the adsorbate. The surface electron cooling time due to electron–phonon coupling and electron diffusion is 1–3 ps [2,5,9,10]. The observed 0.1 ns decay time of the wings, however, provides new information. It indicates that the excitation lasts longer than the electron–adsorbate [10,16], electron–lattice [2,5,9–11], and lattice–adsorbate [24] relaxation times. The only remaining equilibration process is the cooling of the surface to the bulk, which occurs on roughly the same time-scale as the decay of the wings.

To quantify the nonlinear dependence of the yield on fluence we analyzed the depletion curves using a phenomenological model. Our analysis takes into account how the spatial distribution of O_2 on the surface changes with successive laser pulses. For laser pulse i at a given fluence, the desorption profile on the surface is modeled by

$$y_i(\boldsymbol{r}, F_i) = \gamma F_i^p(\boldsymbol{r})\,\theta_i(\boldsymbol{r}), \tag{2}$$

where γ is a proportionality constant, $F_i^p(\boldsymbol{r})$ is the spatial fluence profile of laser pulse i raised to the power p [1–5,9], and $\theta_i(\boldsymbol{r})$ represents the O_2 coverage profile. Successive profiles are obtained from

$$\theta_i(\boldsymbol{r}, \{F_0, F_1, \ldots, F_i\}) = \theta_0 - \sum_{j<i} y_j(\boldsymbol{r}, F_j), \tag{3}$$

with $\theta_0(\boldsymbol{r}) = \theta_0$ the initial uniform coverage. The spatially integrated yield measured by the mass spectrometer is

$$Y_i(\{F_0, F_1, \ldots, F_i\}) = N_0 \int y_i(\boldsymbol{r}, F_i)\, \mathrm{d}\boldsymbol{r}, \tag{4}$$

where N_0 scales the model to the actual data. Each set of depletion curves collected at a given wavelength and pulse duration is fit simultaneously over the entire range of fluences, except for the data at 267 nm. For each species the fitting of a set of depletion curves to Eq. (4) is done by adjusting N_0, γ, and p. Figs. 1 and 2 show that this fitting procedure accommodates the depletion curves and the first shot yields. According to Eqs. (2)–(4) the dependence of the first shot yield on fluence is

$$\frac{Y_0}{\pi ab} = \frac{N_0\theta_0}{p}\gamma F_0^p. \tag{5}$$

The curves in Fig. 2 show the dependence of the first shot yield on fluence using the values for N_0, γ, and

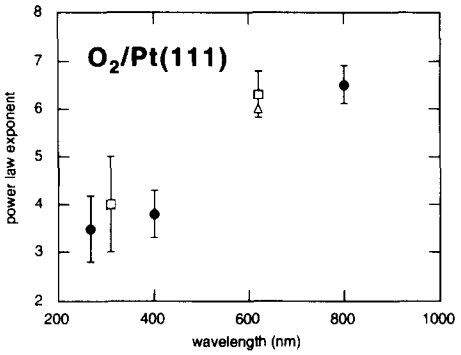

Fig. 5. Wavelength dependence of the power law exponent p, showing the results from this work (●), from Refs. [3,4,25] (□) for O_2/Pt(111), and from Ref. [5] for O_2/Pd(111) (△) [5]. The strong wavelength dependence indicates that nonthermalized electrons play a central role in the ultrafast desorption mechanism.

p obtained from the fit to the respective data sets. The ratio of N_O for O_2 and CO_2 is 10 ± 2, reflecting the difference in yield mentioned earlier. The desorption and reaction data at 267 nm (Fig. 3) were fit by a simple power law, $Y_O \propto E^p$, to the first shot yields alone. Values for the exponent p obtained from the fits are shown in Fig. 5 along with data obtained by others at 310 and 620 nm [3–5,25]. The exponent p decreases with decreasing wavelength and is nearly independent of pulse width at 800 nm.

The yield saturates when the first laser shot completely removes the adsorbate layer in the center of the profile. Saturation occurs at fluences $F_0 \geq F_{sat}$ where $\gamma F_{sat}^p \equiv 1$. Above F_{sat} the factor γF_0^p in Eq. (5) becomes $\ln(\gamma F_0^p) + 1$. The saturation of the curves in Fig. 2 allows us to determine the maximum efficiency of the desorption which occurs at the saturation fluence. At 800 nm $F_{sat} \approx 100$ μJ/mm^2, which means that about $(5 \pm 1) \times 10^{12}$ molecules/mm^2 are desorbed by 4×10^{14} absorbed photons/mm^2. This implies a desorption efficiency of about 1%, several orders of magnitude greater than that reported for nanosecond and continuous irradiation [3,7,26,27].

Summarizing, the following observations emerge from these experiments.

(1) Comparison of data obtained at different wavelengths show a clear dependence of desorption yield on wavelength. This behavior cannot be adequately described by current theoretical models, which predict a dependence on absorbed fluence but not on wavelength. The observed wavelength dependence therefore calls for models that incorporate nonthermal electron distributions.

(2) The desorption yield decreases sharply with increasing pulse duration, but the power law exponent remains nearly the same. Changes in the pulse duration affect the competition between the excitation rate and the thermalization and cooling processes. An increase in pulse duration will result in a lower nonthermalized electron density and a lower electron temperature. Both of these effects could contribute to a decrease in the observed yield.

(3) In addition to the 1.8 ps central peak, the two-pulse experiments show a 0.1 ns decay time exceeding all relaxation times except the cooling of the surface to the bulk temperature. The observation of a two-pulse correlation signal on such a long time scale implies that the temperature of the surface plays a role in the femtosecond-laser-induced desorption process.

(4) The observed saturation of the desorption enables us to estimate the maximum quantum efficiency of the O_2 desorption: 10^{-2} molecule/photon at an absorbed fluence of 100 μJ/mm^2.

This research is supported by the Army Research Office under Contract DAAL03-92-G-0238 and the Joint Services Electronics Program under Contract N00014-89-J-1023. RJF is supported by the Natural Science and Engineering Research Council of Canada. JRG acknowledges support from AASERT Fellowship DAAL03-92-G-0196. Generous support from Perkin–Elmer Physical Electronics, and ConOptics Inc. is gratefully acknowledged.

References

[1] J.A. Prybyla, T.F. Heinz, J.A. Misewich, M.M.T. Loy and J.H. Glownia, Phys. Rev. Letters 64 (1990) 1537.
[2] F. Budde, T.F. Heinz, M.M.T. Loy, J.A. Misewich, F. de Rougemont and H. Zacharias, Phys. Rev. Letters 66 (1991) 3024.
[3] F.-J. Kao, D.G. Busch, D. Gomes da Costa and W. Ho, Phys. Rev. Letters 70 (1993) 4098.
[4] F.-J. Kao, D.G. Busch, D. Cohen, D. Gomes da Costa and W. Ho, Phys. Rev. Letters 71 (1993) 2094.
[5] J.A. Misewich, A. Kalamarides, T.F. Heinz, U. Höfer and M.M.T. Loy, J. Chem. Phys. 100 (1994) 736.
[6] W.D. Mieher and W. Ho, J. Chem. Phys. 91 (1989) 2755.

[7] W.D. Mieher and W. Ho, J. Chem. Phys. 99 (1993) 9279.
[8] V.A. Ukraintsev and I. Harrison, J. Chem. Phys. 96 (1992) 6307.
[9] J.A. Prybyla, H.W.K. Tom and G.D. Aumiller, Phys. Rev. Letters 68 (1992) 503.
[10] F. Budde, T.F. Heinz, A. Kalamarides, M.M.T. Loy and J.A. Misewich, Surface Sci. 283 (1993) 143.
[11] S.I. Anisimov, B.L. Kapeliovich and T.L. Perel'man, Soviet Phys. JETP 39 (1974) 375.
[12] R.W. Schoenlein, W.Z. Lin, J.G. Fujimoto and G.L. Eesley, Phys. Rev. Letters 58 (1987) 1680.
[13] H.E. Elsayedali, T.B. Norris, M.A. Pessot and G.A. Mourou, Phys. Rev. Letters 58 (1987) 1212.
[14] P.B. Corkum, F. Brunel, N.K. Sherman and T. Srinivasan-Rao, Phys. Rev. Letters 61 (1988) 2886.
[15] R.R. Cavanagh, D.S. King, J.C. Stephenson and T.F. Heinz, J. Phys. Chem. 97 (1993) 786.
[16] J.A. Misewich, T.F. Heinz and D.M. Newns, Phys. Rev. Letters 68 (1992) 3737.
[17] D.M. Newns, T.F. Heinz and J.A. Misewich, Progr. Theoret. Phys. Suppl. No. 106 (1991) 411.
[18] T. Matsushima, Surface Sci. 123 (1982) L663.
[19] T. Matsushima, Surface Sci. 127 (1983) 403.
[20] K.-H. Allers, H. Pfnür, P. Feulner and D. Menzel, J. Chem. Phys. 100 (1994) 3985.
[21] H. Steininger, S. Lehwald and H. Ibach, Surface Sci. 123 (1982) 1.
[22] J.H. Weaver, C. Krafka, D.W. Lynch and E.E. Koch, Optical properties of metals, Part 1, Physics data (Karlsruhe, Fachinformationszentrum Energie, Physik, Mathematik, 1981).
[23] W.S. Fann, R.H. Storz, H.W.K. Tom and J. Bokor, Phys. Rev. Letters 68 (1992) 2834.
[24] T.A. Germer, J.C. Stephenson, E.J. Heilweil and R.R. Cavanagh, Phys. Rev. Letters 71 (1993) 3327.
[25] D.G. Busch and W. Ho, private communication.
[26] W. Ho, Comments Condens. Mat. Phys. 13 (1988) 293.
[27] X.-L. Zhou, X.-Y. Zhu and J.M. White, Surface Sci. Rept. 13 (1991) 73.